ACS APPLIED MATERIALS & INTERFACES

Research Article

www.acsami.org

High Aspect Ratio PS-*b*-PMMA Block Copolymer Masks for Lithographic Applications

F. Ferrarese Lupi,*[,†] T. J. Giammaria,[†] F. G. Volpe,[†] F. Lotto,[†] G. Seguini,[†] B. Pivac,[‡] M. Laus,[§] and M. Perego[†]

[†]Laboratorio MDM, IMM-CNR, Via C. Olivetti 2, 20864 Agrate Brianza, Monza and Brianza, Italy

[‡]Institut Ruđer Bošković, Bijenička cesta 54, 10000 Zagreb, Croatia

[§]Dipartimento di Scienze e Innovazione Tecnologica (DISIT), Università del Piemonte Orientale "A. Avogadro", Viale T. Michel 11, 15121, Alessandria, Italy

ABSTRACT: The control of the self-assembly (SA) process and nanostructure orientation in diblock copolymer (DBC) thick films is a crucial technological issue. Perpendicular orientation of the nanostructures in symmetric and asymmetric poly(styrene)-*b*-poly(methyl methacrylate) (PS-*b*-PMMA) block copolymer films obtained by means of simple thermal treatments was demonstrated to occur in well-defined thickness windows featuring modest maximum values, thus resulting in low aspect ratio ($h/d < 2$) of the final lithographic mask. In this manuscript, the thickness window corresponding to the perpendicular orientation of the cylindrical structures in asymmetric DBC is investigated at high temperatures (190 °C $\leq T \leq$ 310 °C) using a rapid thermal processing machine. A systematic study of the annealing conditions (temperature and time) of asymmetric PS-*b*-PMMA (M_n = 67.1, polydispersity index = 1.09) films, with thicknesses ranging from 10 to 400 nm, allowed ordered patterns, with a maximum value of orientational correlation length of 350 nm, to be obtained for film thicknesses up to 200 nm. The complete propagation of the cylindrical structures through the whole film thickness in a high aspect ratio PS template ($h/d \approx 7$) is probed by lift-off process. Si nanopillars are obtained having the same lateral ordering and characteristic dimensions of the DBC lithographic mask as further confirmed by grazing-incidence small-angle X-ray scattering experiments.

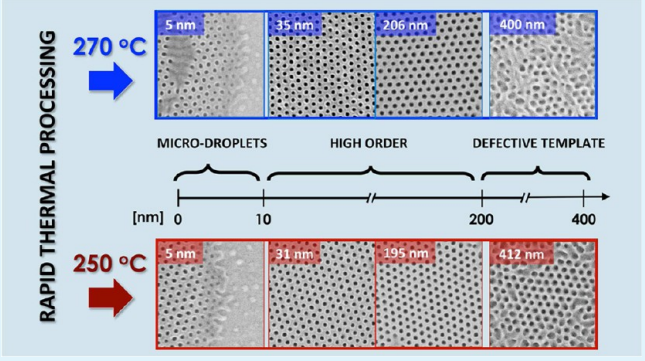

KEYWORDS: *block copolymer, self-assembly, nanolithography, high aspect-ratio, rapid thermal processing, PS-b-PMMA*

1. INTRODUCTION

Among self-assembling (SA) systems, block copolymer thin films have emerged as an attractive cost-effective nanofabrication technology in a number of technological applications, such as separation membranes,[1,2] photovoltaic materials,[3,4] and masks for lithographic applications.[5−7] Because of their inherent tendency to form high-resolution ordered nanostructures, they are commonly used to generate polymeric templates that are integrated in predefined topographical structures, fabricated by means of standard top-down processing techniques, performing a sort of subpatterning of the lithographic structures.[8] The equilibrium structures of the block copolymers are determined by molecular topology, block sequence, composition, molecular size, and the interaction parameters among the chemically distinct block units. In block copolymers with relatively simple architectures, such as AB diblocks and ABA triblocks, the structures include phases with spherical, cylindrical, double gyroid, or lamellar nanostructures, and the natural periodicity of these self-assembled structures is mainly determined by the molar mass of the specific macromolecule under investigation.[9]

Poly(styrene)-*b*-poly(methyl methacrylate) (PS-*b*-PMMA) block copolymers have been proposed as the material of choice for lithographic applications. The possibility of selectively removing one of the two blocks[10] and finely tuning the characteristic size of the nanostructures, up to ∼12 nm,[11,12] allows these diblock copolymers (DBCs) to be used as positive or negative lithographic resists for the patterning of the underlying substrate. In this regard, PS-*b*-PMMA block copolymer thin films, with lamellar and cylindrical structures perpendicularly oriented with respect to the substrate, offer the possibility to fabricate nanometric size wires and pillars having aspect ratios higher than those obtained from parallel cylinders and spheres. Many approaches to direct the orientation of the nanostructures have been proposed so far, including the control of the interfacial interactions between the DBC and the surface through the grafting of homopolymer or random copolymer (RCP) brushes,[13,14] the application of external fields,[15] or by

Received: September 17, 2014
Accepted: November 11, 2014
Published: November 11, 2014

controlling the solvent evaporation rate from the thin film.[16] Among those methods, surface functionalization through the grafting of a PS-*r*-PMMA RCP brush layer has been widely explored in literature.[17−19] However, the perpendicular orientation of both cylindrical and lamellar PS-*b*-PMMA DBC structures, thermally treated at relatively low temperature (170 °C), could be accomplished only in a very limited window of thickness of the block copolymer film, depending on the composition of the underlying random copolymer brush layer.[20] In the best case, the width of the thickness window is restricted to 20 nm and is approximately centered at 30 and 20 nm for cylindrical and lamellar PS-*b*-PMMA block copolymers, respectively. Such thickness constraints imply a significant limitation on the use of the DBCs as lithographic masks, due to the reduced aspect ratio ($h/d \approx 1.5$) of the resulting template. To overcome such limitation, the possible solutions consist in increasing the stiffness of the nanostructured matrix or the film thickness. In the first case alternative approaches such as the sequential infiltration synthesis of DBC[21−23] can guarantee a higher etching contrast with respect to the original PS template. This approach requires the use of the atomic layer deposition (ALD) technique. The second possibility that has been systematically addressed in a recent publication[24] is the fabrication of very thick (h > 100 nm) DBC masks. In ref 24 the perpendicular orientation of PS-*b*-PMMA cylindrical structures has been observed in quite wide thickness window when thermally treating the samples at high temperatures (up to 230 °C). For films thicker than h = 100 nm, the orientation of the structures was observed to be highly dependent on both the annealing temperature and the nature of the two interfaces (i.e., the substrate−polymer interface and the polymer-free surface). It was also observed that the morphological evolution during the thermal treatment of the spun samples depends on the film thickness. In thin films, when h is comparable with the periodicity (L_0), the interaction between the two interfaces is high, so the ordering propagates homogeneously along the film thickness. On the other hand, in thick films ($h \gg L_0$) the two interfaces are decoupled, and the hexagonally packed cylinders originate simultaneously from the top and bottom surfaces with perpendicular orientation with respect to each of them. This mechanism results in the mismatching of the two cylindrical structures propagating independently from the two distinct interfaces. The above interface decoupling occurs approximately in films with h > 300 nm. Nevertheless, even in samples with h < 300 nm, the cylinders appear bended forward with respect to the axis normal to the surface of the film, thus ultimately resulting in a poor propagation through the polymeric mask.[24,25]

An additional limitation to the use of thick DBC films as lithographic masks is the long annealing time required to complete the SA process. Thick films[24] are reported to be annealed for 1.5 h at 230 °C to reach the thermodynamic equilibrium. This annealing time is too long for the process to be integrated in a production line.[26] However, the possibility of completing the SA in thin films within few minutes has been demonstrated by means of fast heating approaches including hot plate[27] and rapid thermal processing (RTP) machine.[28,29] Consequently, the thickness dependence of the DBC ordering using a fast heating technique is worthy of detailed investigation. With this context, the present paper describes the structural characteristics of PMMA cylinders, including the connectivity at both interfaces, in PS-*b*-PMMA films with different thicknesses (between 5 and 400 nm) once the SA process is performed in RTP at different temperatures between 190 and 310 °C, in a reduced amount of time (300 s) compatible with the technological requirements of the production line. The propagation of the cylindrical arrangement within the polymeric film are also delineated by evaporating Si through DBC masks of different thickness.

2. EXPERIMENTAL DETAILS

Sample Preparation. Silicon substrates, with ∼1.8 nm native silicon dioxide (SiO_2) layer, were used as a support for the block copolymer SA. The substrates (∼1 cm^2 surface) were treated with the Piranha solution (H_2SO_4/H_2O_2 with 3/1 v/v ratio at 80 °C for 40 min) to increase the surface density of hydroxyl groups and eliminate any residual organic material. The samples were then rinsed in H_2O and dried under N_2 flow. The hydroxyl end-functionalized P(S-*r*-MMA) copolymer Br-terminated with styrene fraction XS = 0.61, M_n = 14 500 g mol^{-1} and polydispersity index (PDI) = 1.25 was previously synthesized as described in ref 14. Afterward, a P(S-*r*-MMA) solution (18 mg in 2 mL of toluene) was prepared and sonicated in an ultrasonic bath for 300 s. The resulting solution was then spun on the substrates at 3000 rpm for 30 s. The grafting reaction of the P(S-*r*-MMA) chains on the substrate was promoted via thermal treatment performed in RTP at 310 °C for 60 s in a N_2 atmosphere. The nongrafted P(S-*r*-MMA) chains in excess were removed by washing the samples with toluene using an ultrasonic bath. The resultant P(S-*r*-MMA) film is characterized by a thickness of approximately 7 nm.[14]

The asymmetric PS-*b*-PMMA with styrene unit fraction 0.71, average number molecular weight M_n = 67 100 g mol^{-1}, and PDI = 1.09 was purchase from Polymer Source. The PS-*b*-PMMA film thickness was controlled by spin-coating dilute solutions in toluene with different concentrations on the properly neutralized substrates. The DBC thickness was measured by means of a M-200U spectroscopic ellipsometer (J. A. Wollam Co., Inc.) using a xenon lamp at 70° incident angle.

The selective opening of the pores was performed by exposing the samples to UV radiation (5 mW cm^{-2}, exposure time = 900 s) and removing the degraded PMMA in an acetic acid bath for 480 s. Then, an oxygen plasma treatment for 180 s was performed to cross-link the PS chains and remove the random copolymer at the bottom of the pores.

The lift-off process was performed by evaporating a 10 nm thick layer of Si on the nanoporous PS template. Afterward, the polymeric mask was removed by dipping the samples in the Piranha solution at 80 °C for 20 min.

Morphological Analysis. SEM analysis (Zeiss Supra 40 SEM) was performed to evaluate the degree of superficial morphology of the samples. Cross-sectional SEM images were also taken to investigate the complete propagation of the cylindrical structures along the whole film. The calculation of the orientational correlation length (ξ) was performed by processing the several SEM images of the surface of each sample using a Matlab routine, following the process flow described in refs 30 and 31. After a first step of image binarization, the Matlab program localizes the centroids of every cylinder and performs a Delaunay triangulation to determine the coordinates of the vertex of the hexagons. Then the orientational order of the hexagons with respect to the horizontal axis and the associated autocorrelation function (ACF) are calculated. Finally the ξ values were calculated by fitting the ACF with the following equation: ACF = $\exp(-\vec{r}/\xi)$, where $\vec{r}$ is the coordinate vector.

The thickness of the cylindrical Si pillars was obtained by means of grazing-incidence small-angle X-ray scattering (GISAXS) technique. The measurements were carried out in the SAXS beamline of the Elettra-Sincrotrone of Trieste (IT). Data were fitted to pillars of circular cross-section assembled in two-dimensional hexagonal lattice. All the samples were measured at 0.17° (grazing angle), chosen for the strongest scattering intensity and because it is the critical angle of incidence in our system.

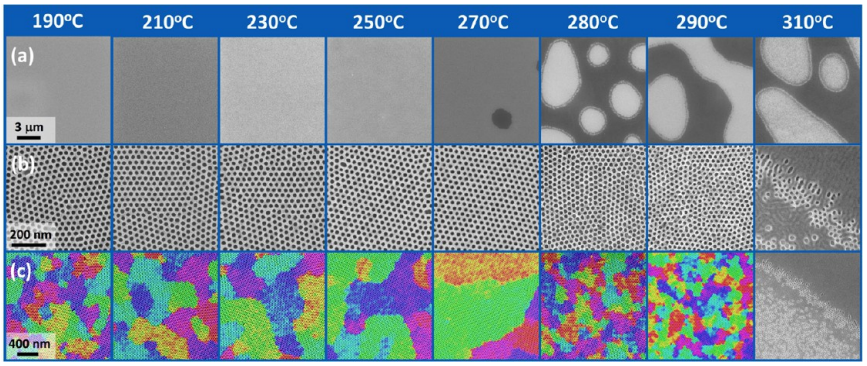

Figure 1. SEM images representing the evolution of the in-plane ordering taken at different magnifications for samples treated at T_a = 190, 210, 230, 250, 270, 280, 290, and 310 °C. The effect of the thermal degradation at $T_a \geq 280$ °C is shown in rows (a, b). In row (c) the color map overlapped with the corresponding SEM images shows the dynamics of the domain coarsening as a function of T_a.

3. RESULTS AND DISCUSSION

Temperature Dependence of Domain Coarsening. The dynamics of domain coarsening and nanostructure orientation in self-assembled PS-*b*-PMMA thin films are strongly influenced by the annealing temperature (T_a) and processing time (t_a).[27,32] High T_a contributes to speed up the kinetics of the system, resulting in a long-range orientational correlation (ξ)[33] and in a significant scaling down of the overall ordering time.[27−29] Nevertheless, there are intrinsic restrictions to the maximum T_a, dictated by the degradation process of the polymeric chains of both random copolymer[32] and block copolymer.[11] Consequently, to identify the best processing conditions, a first set of PS-*b*-PMMA films was prepared by maintaining constant the thickness at $h \approx 35$ nm. Then, the samples were processed in an RTP machine for the fixed annealing time of t_a = 900 s at different temperatures from T_a = 190 to 310 °C. The SEM plan view images of representative samples are reported in Figure 1a,b at two different magnification levels. The samples annealed at $T_a \leq 250$ °C exhibit a perfectly homogeneous morphology with PMMA cylinders perpendicularly oriented with respect to the substrate. For the sample treated at 270 °C, the SEM analysis shows some relatively small areas in which cylindrical nanostructures are no longer visible (dark areas in Figure 1a at T_a = 270 °C). These disorganized areas are highlighted by a different contrast (dark region) in the SEM image of Figure 1a and cover less than 1% of the total area of the sample. By further increasing the annealing temperature (T_a > 270 °C), the DBC films present large disorganized regions over the whole surface of the samples (dark zones in the SEM images of Figure 1a at 280, 290, and 310 °C). On the other hand, the brighter areas represent quite small self-organized portions of the films.

SEM images in Figure 1b depicted a significant variation of the domain size in the block copolymer films depending on the annealing temperature T_a. The quantification of the lateral order was performed by extracting the correlation length values ξ for all the samples, following the procedure reported in literature.[33] For the samples annealed at T_a = 280 and 290 °C, the ξ values were calculated considering only the zones where the nanostructures in the DBC film are perpendicularly oriented with respect to the substrate and the hexagonal arrangement of the PMMA cylinders is visible (brighter zones in the corresponding SEM of Figure 1a). The evolution of the domain coarsening as a function of the annealing temperature is described in Figure 1c, in which the color maps delimiting the domain boundary are located in correspondence with the relevant SEM images. The domain boundaries are located in correspondence with the formation of lattice defects in two-dimensional hexagonal arrays, such as 5-fold or 7-fold dislocations and disclinations.[34]

Figure 2 reports the ξ values as a function of the annealing temperature. The domain size increases with temperature, with

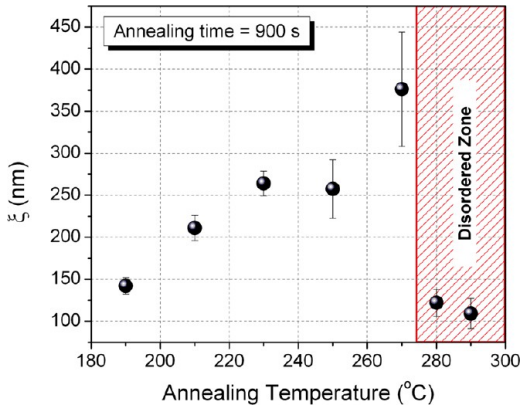

Figure 2. Temperature dependence of the ξ for samples annealed at temperatures between T_a = 190 and 290 °C.

ξ raising from 145 (T_a = 190 °C) to 400 nm (T_a = 270 °C). However, for T_a > 270 °C, a drop of ξ occurs.

Time Evolution. At 270 °C, the polymeric film exhibits the highest correlation length, but some relatively small regions, where the polymer does not properly organize, are present. In contrast, at 250 °C the polymeric film is homogeneously organized, but the correlation length is lower than at 270 °C. For these reasons, in the following experiments, the polymeric films were processed at T_a = 270 °C, corresponding to the highest ξ value, and at T_a = 250 °C, corresponding to the highest temperature at which the sample does not show any sign of degradation of the order.

Once the annealing temperatures T_a were selected, the effect of the annealing time was investigated with the general perspective of exploring a processing window compatible with the technological requirements of a production line.[26] Consequently, two different sets of samples were processed at 250 and 270 °C with annealing time t_a comprised between 10 and 900 s.[28] Figure 3a,b illustrates the plan-view images of the samples annealed for 10, 60, and 300 s at 250 and 270 °C, respectively. Although the presence of perpendicularly organized hexagonally packed structures is evident, a very high

dx.doi.org/10.1021/am506391n | ACS Appl. Mater. Interfaces 2014, 6, 21389−21396

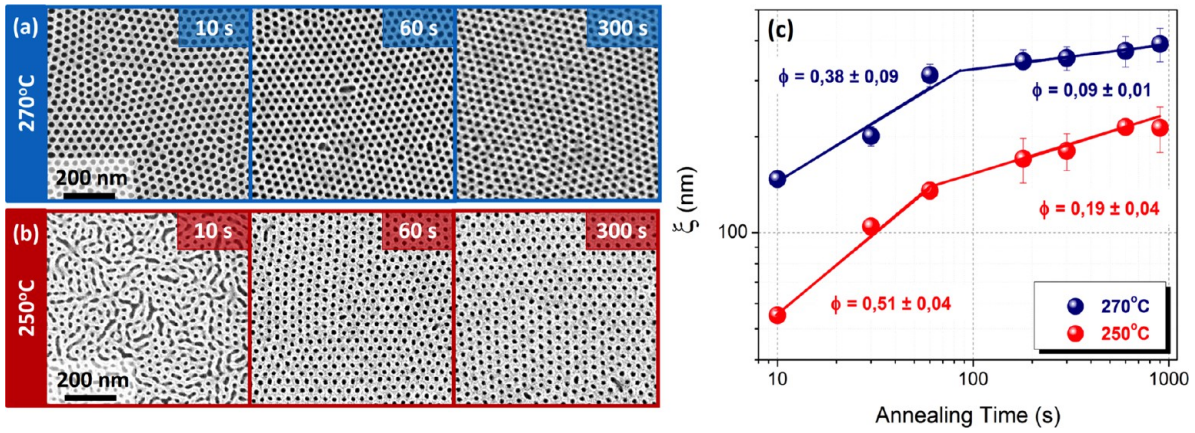

Figure 3. Evolution of the lateral order for samples treated at 250 (a) and 270 °C (b) for different annealing times. (c) Time evolution of the orientational correlation length for the two set of samples annealed at 250 °C (red points) and 270 °C (blue points).

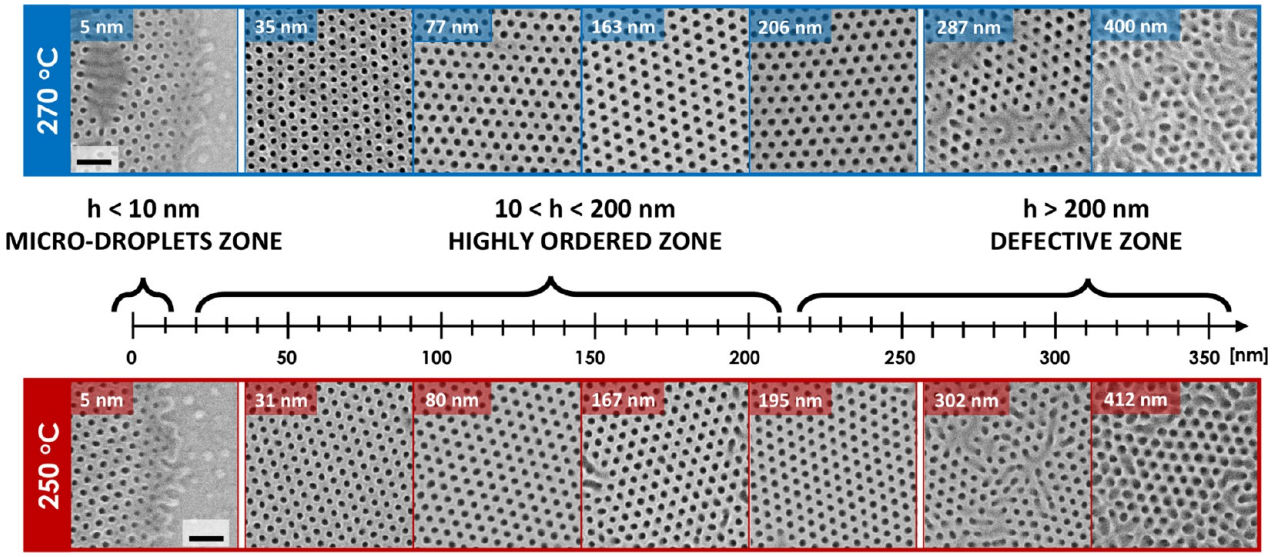

Figure 4. Suface morphology of the DBC samples having different thickness and treated at 270 °C (upper blue row) and 250 °C (lower red row). Three different zones (microdroplets zone, highly ordered zone, and defective zone) are indicated as a function of the film thickness.

density of defects can be seen for the sample annealed at T_a = 250 °C for t_a = 10 s, and a very limited lateral order is observed for the sample annealed at T_a = 270 °C for t_a = 10 s. Conversely, the samples annealed for 60 and 300 s exhibit a well-developed lateral organization with few or no defects in the polymeric matrix. In addition, even operating at T = 270 °C, corresponding to t_a < 600 s, the DBC film does not show any trace of nonorganized zones or inhomogeneity, at variance with the previous observation for the sample prepared at 270 °C for t_a = 900 s.

The ξ values obtained at 250 and 270 °C are reported as a function of annealing time in Figure 3c. The time evolution of ξ presents two distinct coarsening regimes. At both annealing temperatures, the correlation length ξ increases, steeply at first, and then more gradually, with a well-defined threshold at ∼60 s. These two regimes are characterized by power laws with markedly different growth exponent ϕ. For the samples annealed at T_a = 270 °C (blue circles in Figure 3c) the growth exponent of the fast coarsening regime is ϕ_F = 0.38 ± 0.09, while in the slow coarsening regime it is ϕ_S = 0.09 ± 0.01. At T_a = 250 °C the two growth exponents of the fast and slow regimes are ϕ_F = 0.51 ± 0.04 and ϕ_S = 0.19 ± 0.04, respectively. The ϕ values that are measured during the fast coarsening regime are significantly higher than those reported in the literature in the case of cylinder-forming PS-*b*-PMMA block copolymers.[33] The origin of the two distinct ordering regimes is probably related to the presence of some residual solvent retained inside the films during the initial stages of the annealing process, as reported elsewhere.[28,30,31,35] These results demonstrate that in asymmetric PS-*b*-PMMA films the ordering kinetic is significantly enhanced when the self-assembly process is performed at high temperature in an RTP system.

Thickness Dependence. On the basis of the results illustrated in the previous sections, the annealing time t_a = 300 s is assumed to represent a reasonable trade-off between the needs of minimum processing time and maximum degree of lateral order. Consequently, several DBC films with thickness h ranging from 5 to 400 nm were prepared to study the evolution, as a function of h, of the lateral ordering of the nanostructures and the propagation of the PMMA cylinders in the perpendicular direction with respect to the substrate.

Figure 4 reports the SEM plan view images of the samples annealed at 250 (red row) and 270 °C (blue row), as a function of the thickness of the DBC film. Three well-defined thickness

regions are observed. For h < 10 nm, the formation of droplets with diameters in the micrometer range occurs, whereas for film thicknesses between 10 and 200 nm, the polymeric film is homogeneously distributed on the substrate, and wide domains featuring a noticeable level of lateral order are observed. Finally, corresponding to h > 200 nm, the films are still homogeneous, but several defects start to appear at the surface, thus decreasing the average domain size.

In more details, corresponding to thickness h < 10 nm, the surface tension of the DBC is so high that when the film is heated over the glass transition temperature, the microdroplet formation process takes place leading to the formation of polymer droplets on the SiO_2 substrate (Figure 5). For T_a =

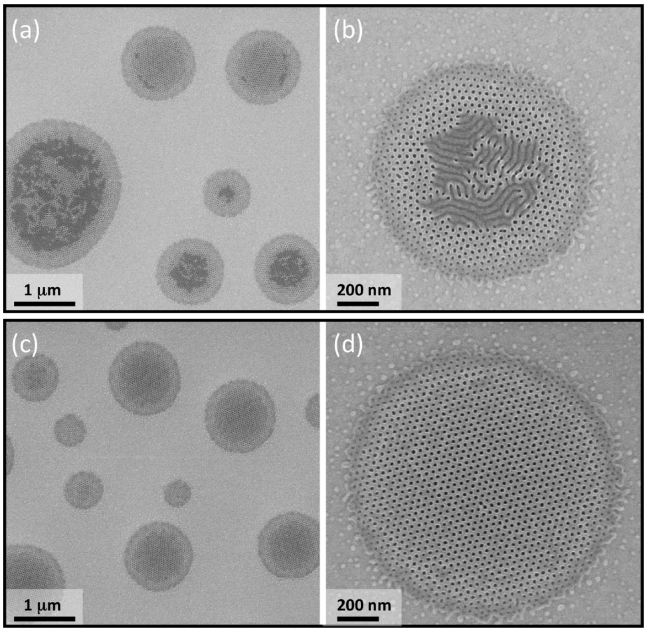

Figure 5. Microdroplet formation from thin DBC films ($h \approx 5$ nm) treated for 300 s at T_a = 270 °C (a, b) and T_a = 250 °C (c, d). Whereas lateral ordering of the cylindrical nanostructures is perfect inside the droplets of the sample annealed at T_a = 250 °C, the formation of some defects in the sample annealed at T_a = 270 °C is observed.

250 °C, the coupling of the circular geometry of the microdroplets with the DBC cylinder structure leads to the formation of a domain in which the hexagonally packed nanostructures own a single orientation (Figure 5d). These well-organized microdroplets can be integrated in a lithographic process flow[36] leading to interesting nanopattern structures. On the other hand, in samples annealed at T_a = 270 °C, the central part of the droplets presents defects, consisting of PMMA bridges among adjacent cylinders or even small parallel cylinders (Figure 5b).

The trend of the correlation length as a function of the film thickness at 250 and 270 °C, is illustrated in Figure 6 for samples with thickness h > 10 nm. The correlation length is practically constant over a wide thickness region with $\xi \sim 180$ nm when the annealing temperature is 250 °C and $\xi \sim 350$ nm when the annealing temperature is 270 °C. For thickness higher than 200 nm, an abrupt decrease in the correlation length occurs at both annealing temperatures. The correlation length reaches a minimum value of $\xi \sim 50$ nm for thick film with $h \sim$ 400 nm irrespective of the annealing temperature.

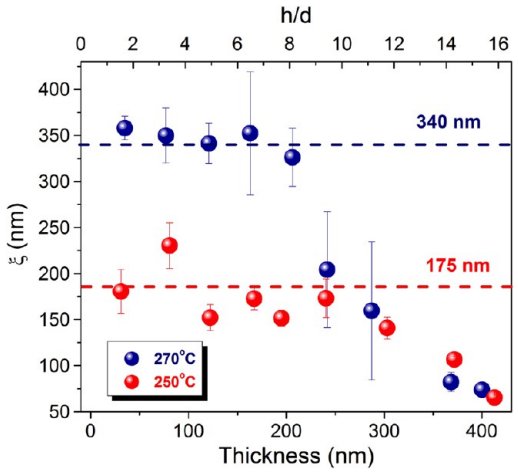

Figure 6. Correlation length ξ as a function of the film thickness for two different sets of samples, annealed at 250 °C (red symbols) and 270 °C (blue symbols). The upper axis reports the aspect ratio h/d corresponding to the film thickness.

To understand the propagation efficiency of cylinders through the film after PMMA removal and to check the effective perpendicular and lateral ordering at the substrate surface, cross-sectional SEM analysis was performed on the samples with thicknesses between 10 and 200 nm. A representative image of the top view and the complementary cross-section of a sample annealed at 270 °C with thickness h = 206 nm is reported in Figure 7a,b, respectively. This sample was chosen since it is the thicker sample in the constant correlation length region. Clear evidence of the propagation of the cylinders along the whole film thickness is given by SEM analysis performed in a zone of the sample in which the film is peeled. In these zones the DBC layer is detached from the SiO_2, forming a sort of spatial undulation over the substrate under which the substrate−DBC interface is exposed (represented in Figure 7c). SEM analysis performed under the peeled DBC film revealed the same hexagonal arrangement of the cylinders perpendicular to the interface between the DBC and the free surface also in the bottom part of the film (see Figure 7d). The main problem preventing a systematic use of this approach to investigate the organization of the film through the entire thickness of the film is that cross-sectional SEM imaging allows studying the perpendicular orientation of the nanostructures only at a local scale. To prove the vertical orientation of the nanostructures on a large scale an alternative approach is required.

Therefore, the propagation of the hexagonal pattern through the whole film thickness can be effectively probed by a lift-off process. After selective removal of the PMMA phase, a 10 nm thick layer of Si was evaporated on the remaining nanoporous PS template and through the nanopores. Figure 8 reports the SEM plan view images of the Si pillars that are formed on the SiO_2 substrate after the complete removal of the DBC mask. For films with thicknesses between 20 and 170 nm (Figures 8a−c), the formation of hexagonally packed Si pillars that perfectly replicate the original PS template is observed. As reported by other authors,[37] the presence on the surface of Si pillars having widely different diameter and of small pillars with elliptical shape in the sample having h = 206 nm (Figure 8d) could be ascribed to the bending of the cylinders with respect to the vertical axes observed in the SEM images (Figure 7d).

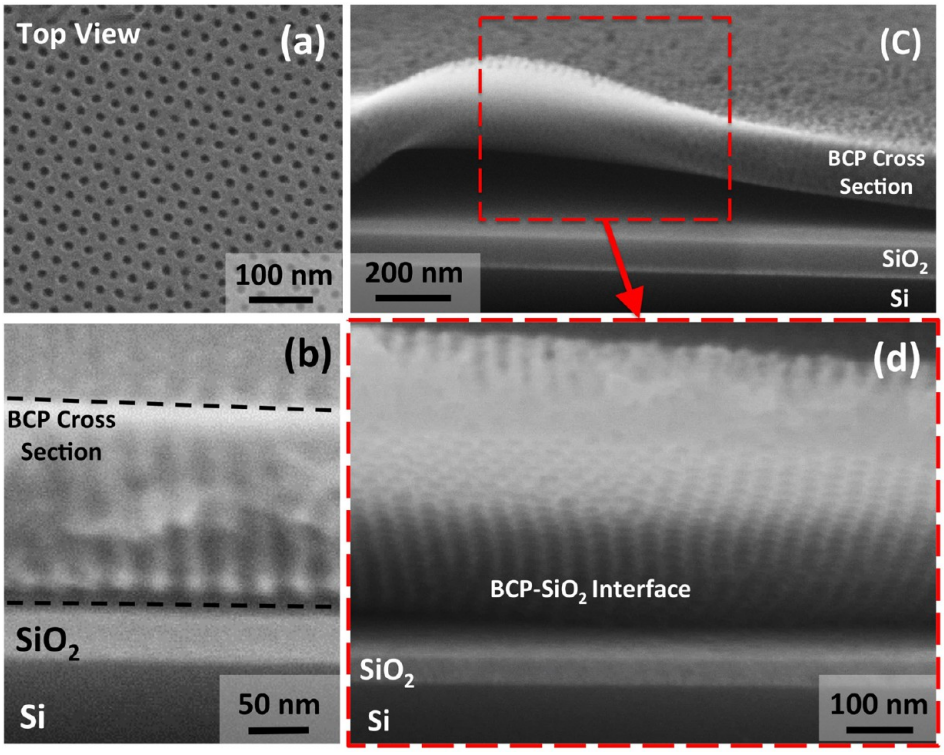

Figure 7. SEM images representing the top view (a) and the cross-section (b) of 206 nm thick sample. (c) The peeled zone of the sample is represented. (d) A zoomed view of the inferior part of the peeled zone, corresponding to the dashed rectangle indicated in (c).

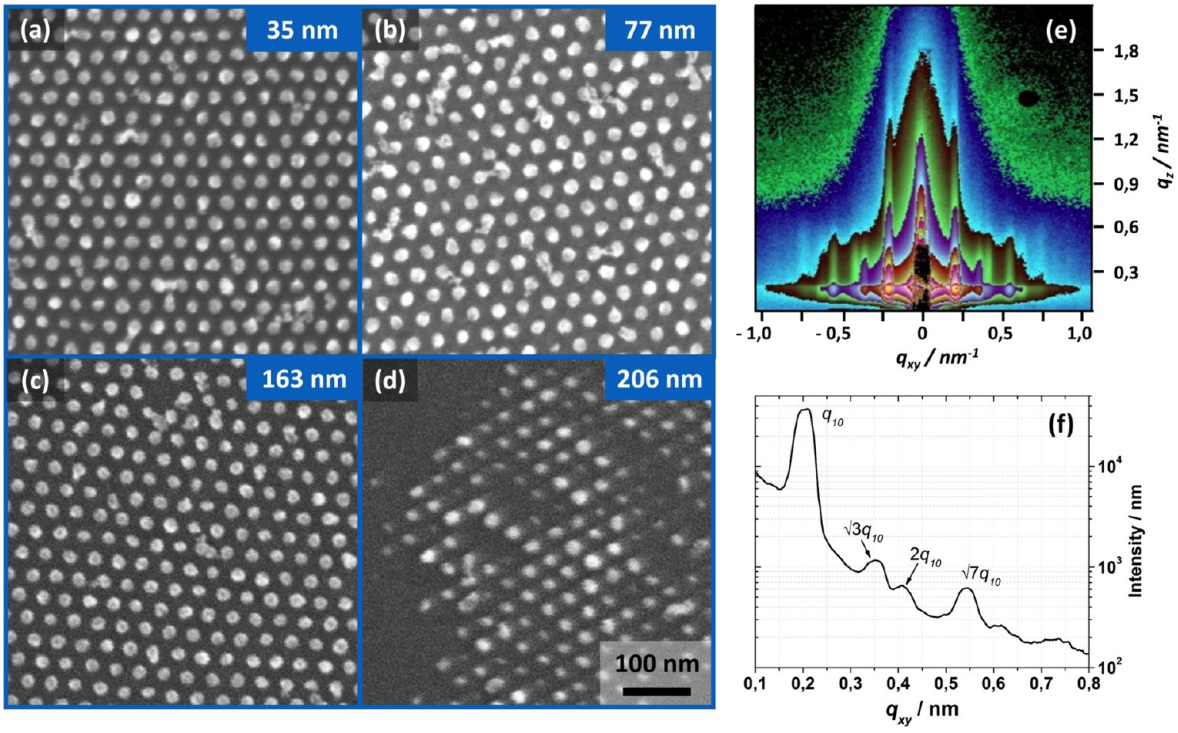

Figure 8. SEM images representing the Si pillars obtained by lift-off process through DBC mask annealed at 270 °C of thickness h = 35 nm (a), 77 nm (b), 163 nm (c), and 206 nm (d). (e) GISAXS pattern corresponding to Si pillars of 10 nm height. (f) Horizontal intensity profiles measured along q_z = 0.22 nm^{-1} at an incidence angle α_i = 0.17°.

To provide additional information on the height of the nanometric pillars and their characteristic dimensions (diameter d and lattice spacing L_0), GISAXS experiments were performed on a representative set of samples. In Figure 8e is reported the GISAXS pattern corresponding to the sample in Figure 8b. The measured height of the Si pillars (h = 11 ± 3) is compatible with the nominal value of Si evaporated through the DBC mask, that is, 10 nm. The lattice spacing extracted from the

dx.doi.org/10.1021/am506391n | ACS Appl. Mater. Interfaces 2014, 6, 21389−21396

GISAXS spectrum (L_0 = 37 ± 2 nm), calculated from the position of the q_{10} vector (Figure 8f) following the relation $L_0 = 4\pi\sqrt{3}q_{10}$ and the diameter of the pillars d = 24 ± 3 nm are in good agreement with the characteristic dimensions of the initial DBC mask calculated by the SEM analysis (L_0 = 35 ± 1 nm and d = 23.8 ± 1.4 nm), further confirming the good quality of the polymeric mask and the effective propagation of the PMMA cylinders through the entire thickness of the polymeric film.

The described experiment demonstrates the possibility of controlling the self-assembly of DBC film on RCP neutralized substrates to fabricate hexagonally packed PMMA cylinders in a PS templates, having h values lying well outside the thickness window reported in refs 17−19. Interestingly, these results are obtained using an extremely simple thermal treatment, without any further constraint to direct the orientation of the cylindrical structures, such as the application of a DC electric field,[15] the addition of PMMA homopolymer to the DBC,[38] or the deposition of the DBC on indium tin oxide substrates having random roughness.[25,39] However, in spite of the high aspect ratio obtainable with those alternative methods, the excessive bending of the nanostructures showed by the cross-sectional SEM and TEM images, which are reported in the aforecited works, prevents the effective use of these thick PS-*b*-PMMA films as lithographic mask.

Very few data on the orientation of PS-*b*-PMMA nanostructures in thick films exclusively by thermal treatments are reported in literature.[33] In this specific case, the experiments were carried out at $T_a \leq 230$ °C and showed a decoupling between the two interfaces of the thick polymeric films with the substrate and the air, respectively, leading to the formation of two independent and disconnected fronts of PMMA cylinders propagating from the two interfaces and exhibiting extremely high ξ values. Even in this case, the use of the thick nanoporous PS template as nanolithographic tool was excluded due to the bending of the PMMA cylinders within the film and to the formation of the discontinuities between the two propagating fronts. For this reason the authors exploited the molecular transfer printing technique to replicate the highly ordered pattern.

The experimental procedure reported by Ji et al. and the one adopted in the present manuscript exhibit significant differences, consisting in the high annealing temperature (T_a = 250 or 270 °C), the controlled N_2 atmosphere, and the overall duration of the annealing treatment. Under the present experimental conditions, the perpendicular orientation of the cylinders through the whole film for sample with $h \leq 170$ nm is promoted in short (i.e., 300 s), which is compatible with requirements. The direct consequence of such achievement is the possibility of tuning the aspect ratio of the resulting PS mask over a quite broad range of values, providing the opportunity to optimize the thickness of the polymeric mask as a function of the requirements of the specific process under development. In particular, the range of the accessible aspect ratios is extended from the value $h/d < 2$, which is commonly reported for DBC films annealed in conventional furnaces/ovens, to $h/d \approx 7$, for samples annealed in RTP, reducing at the same time the duration of the thermal treatment. This result represents an important breakthrough in the exploitation of DBC-based lithography, increasing the flexibility of this self-assembly lithographic strategy and removing one of the bottlenecks that limit the integration of these materials in conventional nanofabrication process flow.

4. CONCLUSIONS

The lateral ordering and vertical orientation of the PMMA cylinders in PS-*b*-PMMA films with different thicknesses (between 5 and 400 nm) when annealed at high temperature (190 °C ≤ T_a ≤ 310 °C) have been systematically investigated. After identification of the highest processing temperature for this specific polymeric system (T_a = 270 °C), it has been demonstrated that, in a limited temporal scale (t_a < 300 s), the lateral ordering of the cylindrical structures remains constant in the whole window of thickness under investigation (10 < h < 200 nm), resulting in hexagonally packed PMMA cylinders embedded in a PS matrix. A lift-off process performed by evaporating Si through the high aspect ratio DBC masks confirmed the effective propagation of the perpendicular orientation of the PMMA cylinders through the entire film until h < 170 nm. As a result of this study, the thickness window for the perpendicular orientation of the nanostructures has been extended, fabricating PS template having an aspect ratio having a maximum aspect ratio of $h/d \approx 7$ and with orientational correlation length as high as $\xi \approx 350$ nm.

AUTHOR INFORMATION

Corresponding Author

*E-mail: federico.ferrareselupi@mdm.imm.cnr.it.

Notes

The authors declare no competing financial interest.

ACKNOWLEDGMENTS

This research activity was funded by the EMRP Joint Research Project SiB61 CRYSTAL. Patent protection related to this work is pending. We also acknowledge S. Grasso at ST-Microelectronics for fruitful discussions.

REFERENCES

(1) Yang, S. Y.; Ryu, I.; Kim, H. Y.; Kim, J. K.; Jang, S. K.; Russell, T. P. Nanoporous Membranes with Ultrahigh Selectivity and Flux for the Filtration of Viruses. *Adv. Mater.* **2006**, *18*, 709−712.

(2) Phillip, W. A.; O'Neill, B.; Rodwogin, M.; Hillmyer, M. A.; Cussler, E. L. Self-Assembled Block Copolymer Thin Films as Water Filtration Membranes. *ACS Appl. Mater. Interfaces* **2010**, *2*, 847−853.

(3) Guo, C.; Lin, Y. H.; Witman, M. D.; Smith, K.; Wang, C.; Hexemer, A.; Strzalka, J.; Gomez, E. D.; Verduzco, R. Conjugated Block Copolymer Photovoltaics with Near 3% Efficiency Through Microphase Separation. *Nano Lett.* **2013**, *13*, 2957−2963.

(4) Darling, S. B. Block Copolymers for Photovoltaics. *Energy Environ. Sci.* **2009**, *2*, 1266.

(5) Bates, C. M.; Maher, M. J.; Janes, D. W.; Ellison, C. J.; Willson, C. G. Block Copolymer Lithography. *Macromolecules* **2014**, *47*, 2−12.

(6) Black, C. T.; Ruiz, R.; Breyta, G.; Cheng, J. Y.; Colburn, M. E.; Guarini, K. W.; Zhang, Y.; Heights, Y. Polymer Self Assembly in Semiconductor Microelectronics. *IBM J. Res. Dev.* **2007**, *51*, 605−633.

(7) Bang, J.; Jeong, U.; Ryu, D. Y.; Russell, T. P.; Hawker, C. J. Block Copolymer Nanolithography: Translation of Molecular Level Control to Nanoscale Patterns. *Adv. Mater.* **2009**, *21*, 4769−4792.

(8) Darling, S. B. Directing the Self-Assembly of Block Copolymers. *Prog. Polym. Sci.* **2007**, *32*, 1152−1204.

(9) Bates, F. S. Polymer-Polymer Phase Behavior. *Science* **1991**, *251*, 898.

(10) Darling, S. B.; Yufa, N.; Cisse, A. L.; Bader, S. D.; Sibener, S. J. Self-Organization of FePt Nanoparticles on Photochemically Modified Diblock Copolymer Templates. *Adv. Mater.* **2005**, *17*, 2446−2450.

(11) Ferrarese Lupi, F.; Giammaria, T. J.; Seguini, G.; Vita, F.; Francescangeli, O.; Sparnacci, K.; Antonioli, D.; Gianotti, V.; Laus, M.; Perego, M. Fine Tuning of Lithographic Masks through Thin Films of

PS-b-PMMA with Different Molar Mass by Rapid Thermal Processing. *ACS Appl. Mater. Interfaces* **2014**, *6*, 7180−7188.
(12) Xu, T.; Kim, H.; Derouchey, J.; Seney, C.; Levesque, C.; Martin, P.; Stafford, C. M.; Russell, T. P. The Influence of Molecular Weight on Nanoporous Polymer Films. *Polymer* **2001**, *42*, 9091−9095.
(13) Guo, R.; Kim, E.; Gong, J.; Choi, S.; Ham, S.; Ryu, D. Y. Perpendicular Orientation of Microdomains in PS-b-PMMA Thin Films on the PS Brushed Substrates. *Soft Matter* **2011**, *7*, 6920.
(14) Ferrarese Lupi, F.; Giammaria, T. J.; Seguini, G.; Ceresoli, M.; Perego, M.; Antonioli, D.; Gianotti, V.; Sparnacci, K.; Laus, M. Flash Grafting of Functional Random Copolymers for Surface Neutralization. *J. Mater. Chem. C* **2014**, *2*, 4909−4917.
(15) Thurn-Albrecht, T. Ultrahigh-Density Nanowire Arrays Grown in Self-Assembled Diblock Copolymer Templates. *Science* **2000**, *290*, 2126−2129.
(16) Phillip, W.; Hillmyer, M.; Cussler, E. L. Cylinder Orientation Mechanism in Block Copolymer Thin Films Upon Solvent Evaporation. *Macromolecules* **2010**, *43*, 7763−7770.
(17) Ryu, D. Y.; Shin, K.; Drockenmuller, W.; Hawker, C. J.; Russell, T. P. A Generalized Approach to the Modification of Solid Surfaces. *Science* **2005**, *308*, 236.
(18) Mansky, P.; Liu, Y.; Huang, E.; Russell, T. P.; Hawker, C. Controlling Polymer-Surface Interactions with Random Copolymer Brushes. *Science* **1997**, *275*, 1458.
(19) Andreozzi, A.; Poliani, E.; Seguini, G.; Perego, M. The Effect of Random Copolymer on the Characteristic Dimensions of Cylinder-Forming PS-b-PMMA Thin Films. *Nanotechnology* **2011**, *22*, 185304.
(20) Ham, S.; Shin, C.; Kim, E.; Ryu, D. Y.; Jeong, U.; Russell, T. P.; Hawker, C. J. Microdomain Orientation of PS-b-PMMA by Controlled Interfacial Interactions. *Macromolecules* **2008**, *41*, 6431−6437.
(21) Peng, Q.; Tseng, Y.-C.; Darling, S. B.; Elam, J. W. Nanoscopic Patterned Materials with Tunable Dimensions via Atomic Layer Deposition on Block Copolymers. *Adv. Mater.* **2010**, *22*, 5129−5133.
(22) Tseng, Y.-C.; Peng, Q.; Ocola, L. E.; Elam, J. W.; Darling, S. B. Enhanced Block Copolymer Lithography Using Sequential Infiltration Synthesis. *J. Phys. Chem. C* **2011**, *115*, 17725−17729.
(23) Tseng, Y.-C.; Peng, Q.; Ocola, L. E.; Czaplewski, D. A.; Elam, J. W.; Darling, S. B. Etch Properties of Resists Modified by Sequential Infiltration Synthesis. *J. Vac. Sci. Technol., B* **2011**, *29*, 6.
(24) Han, E.; Stuen, K. O.; Leolukman, M.; Liu, C.-C.; Nealey, P. F.; Gopalan, P. Perpendicular Orientation of Domains in Cylinder-Forming Block Copolymer Thick Films by Controlled Interfacial Interactions. *Macromolecules* **2009**, *42*, 4896−4901.
(25) Sivaniah, E.; Hayashi, Y.; Matsubara, S.; Kiyono, S.; Hashimoto, T.; Fukunaga, K.; Kramer, E. J.; Mates, T. Symmetric Diblock Copolymer Thin Films on Rough Substrates. Kinetics and Structure Formation in Pure Block Copolymer Thin Films. *Macromolecules* **2005**, *38*, 1837−1849.
(26) International Technology Roadmap for Semiconductors (ITRS), Emerging Research Materials 2011.
(27) Welander, A. M.; Kang, H.; Stuen, K. O.; Solak, H. H.; Müller, M.; De Pablo, J. J.; Nealey, P. F. Rapid Directed Assembly of Block Copolymer Films at Elevated Temperatures. *Macromolecules* **2008**, *41*, 2759−2761.
(28) Ferrarese Lupi, F.; Giammaria, T. J.; Ceresoli, M.; Seguini, G.; Sparnacci, K.; Antonioli, D.; Gianotti, V.; Laus, M.; Perego, M. Rapid Thermal Processing of Self-Assembling Block Copolymer Thin Films. *Nanotechnology* **2013**, *24*, 315601.
(29) Seguini, G.; Giammaria, T. J.; Ferrarese Lupi, F.; Sparnacci, K.; Antonioli, D.; Gianotti, V.; Vita, F.; Placentino, I. F.; Hilhorst, J.; Ferrero, C.; Francescangeli, O.; Laus, M.; Perego, M. Thermally Induced Self-Assembly of Cylindrical Nanodomains in Low Molecular Weight PS-b-PMMA Thin Films. *Nanotechnology* **2014**, *25*, 045301.
(30) Harrison, C.; Angelescu, D. E.; Trawick, M.; Cheng, Z.; Huse, D.; Chaikin, P. M.; Vega, D.; Sebastian, J. M.; Register, R.; Adamson, D. H. Pattern Coarsening in a 2D Hexagonal System. *Europhys. Lett.* **2004**, *67*, 800−806.
(31) Vega, D.; Harrison, C.; Angelescu, D.; Trawick, M.; Huse, D.; Chaikin, P.; Register, R. Ordering Mechanisms In Two-Dimensional Sphere-Forming Block Copolymers. *Phys. Rev. E* **2005**, *71*, 061803.
(32) Ceresoli, M.; Ferrarese Lupi, F.; Seguini, G.; Sparnacci, K.; Gianotti, V.; Antonioli, D.; Laus, M.; Boarino, L.; Perego, M. Evolution of Lateral Ordering in Symmetric Block Copolymer Thin Films Upon Rapid Thermal Processing. *Nanotechnology* **2014**, *25*, 275601.
(33) Ji, S.; Liu, C.; Liao, W.; Fenske, A. L.; Craig, G. S. W.; Nealey, P. F. Domain Orientation and Grain Coarsening in Cylinder-Forming Poly (styrene-b-methyl methacrylate) Films. *Macromolecules* **2011**, *44*, 4291−4300.
(34) Hammond, M. R.; Sides, S. W.; Fredrickson, G. H.; Kramer, E. J. Adjustment of Block Copolymer Nanodomain Sizes at Lattice Defect Sites. *Macromolecules* **2003**, *36*, 8712−8716.
(35) Perego, M.; Ferrarese Lupi, F.; Ceresoli, M.; Giammaria, T. J.; Seguini, G.; Enrico, E.; Boarino, L.; Antonioli, D.; Gianotti, V.; Sparnacci, K.; Laus, M. Ordering Dynamics in Symmetric PS-b-PMMA Diblock Copolymer Thin Films During Rapid Thermal Processing. *J. Mater. Chem. C* **2014**, *2*, 6655−6664.
(36) Farrell, R. A.; Kehagias, N.; Shaw, M. T.; Reboud, V.; Zelsmann, M.; Holmes, J. D.; Sotomayor Torres, C. M.; Morris, M. A. Surface-Directed Dewetting of a Block Copolymer for Fabricating Highly Uniform Nanostructured Microdroplets and Concentric Nanorings. *ACS Nano* **2011**, *5*, 1073−1085.
(37) Bosworth, J. K.; Dobisz, E. A.; Hellwig, O.; Ruiz, R. Impact of Out-of-Plane Translational Order in Block Copolymer Lithography. *Macromolecules* **2011**, *44*, 9196−9204.
(38) Jeong, U.; Ryu, D. Y.; Kho, D. H.; Kim, J. K.; Goldbach, J. T.; Kim, D. H.; Russell, T. P. Enhancement in the Orientation of the Microdomain in Block Copolymer Thin Films Upon the Addition of Homopolymer. *Adv. Mater.* **2004**, *16*, 533−536.
(39) Tsori, Y.; Sivaniah, E.; Andelman, D.; Hashimoto, T. Orientational Transitions in Symmetric Diblock Copolymers on Rough Surfaces. *Macromolecules* **2005**, *38*, 7193−7196.